Peer-reviewed version available at *Cancers* **2019**, *11*, 1905; doi:10.3390/cancers11121905

Article

Genomic landscape of patient-matched tumor and circulating cell-free DNA in metastatic melanoma

Russell J. Diefenbach [1,2], Jenny H. Lee [1,2], Dario Strbenac [3], Jean Y. H. Yang [3,4], Alexander M. Menzies [2,5,7], Matteo S. Carlino [2,5,6], Georgina V. Long [2,4,5,7], Andrew J. Spillane [2,5,7], Jonathan R. Stretch [2], Robyn P. M. Saw [2,5,8], John F. Thompson [2,5,8], Sydney Ch'ng [2,5], Richard A. Scolyer [2,4,5,9], Richard F. Kefford [2,5,10], and Helen Rizos [1,2]*.

[1] Department of Biomedical Sciences, Faculty of Medicine and Health Sciences, Macquarie University, Sydney, NSW, Australia; russell.diefenbach@mq.edu.au (R.J.D.); jenny.lee@mq.edu.au (J.H.L.); helen.rizos@mq.edu.au (H.R.)
[2] Melanoma Institute Australia, The University of Sydney, Sydney, NSW, Australia; jonathan.stretch@melanoma.org.au (J.R.S.); robyn.saw@melanoma.org.au (R.P.M.S.); john.thompson@melanoma.org.au (J.F.T.)
[3] School of Mathematics and Statistics, The University of Sydney, Sydney, NSW, Australia dario.strbenac@sydney.edu.au (D.S.); jean.yang@sydney.edu.au (J.Y.H.Y)
[4] Charles Perkins Centre, The University of Sydney, Sydney, NSW, Australia
[5] Sydney Medical School, The University of Sydney, Sydney, NSW, Australia; alexander.menzies@sydney.edu.au (A.M.M.); matteo.carlino@sydney.edu.au (M.S.C.); georgina.long@sydney.edu.au (G.V.L.); andrew.spillane@sydney.edu.au (A.J.S.); sydney.chng@sydney.edu.au (S.C.)
[6] Crown Princess Mary Cancer Centre, Westmead and Blacktown hospitals, Sydney, NSW, Australia
[7] Department of Medical Oncology, Northern Sydney Cancer Centre, Royal North Shore Hospital, Sydney, NSW, Australia
[8] Department of Melanoma and Surgical Oncology, Royal Prince Alfred Hospital, Sydney, NSW, Australia
[9] Department of Tissue Pathology and Diagnostic Oncology, Royal Prince Alfred Hospital, Sydney, NSW, Australia richard.scolyer@health.nsw.gov.au (R.A.S)
[10] Department of Clinical Medicine, Faculty of Medicine and Health Sciences, Macquarie University, Sydney, NSW, Australia; richard.kefford@mq.edu.au (R.F.K.)
* Correspondence: helen.rizos@mq.edu.au; Tel.: +61-2-9850-2762

Abstract: The use of circulating cell-free (cf) DNA to monitor cancer progression and response to therapy has significant potential but there is only limited data on whether this technique can detect the presence of low frequency subclones that may ultimately confer therapy resistance. In this study, we sought to evaluate whether whole-exome sequencing of cfDNA can accurately profile the mutation landscape of metastatic melanoma. We used whole-exome sequencing (WES) to identify variants in matched tumor-derived genomic (g) DNA and plasma-derived cfDNA isolated from a cohort of 10 metastatic cutaneous melanoma patients. WES parameters such as sequencing coverage and total sequencing reads were comparable between gDNA and cfDNA. There was significant concordance between gDNA and cfDNA based on the total number of variants identified and the degree of overlap in variants which was independent of the site of tumor biopsy. The mutant allele frequency of common single nucleotide variants was lower in cfDNA reflecting lower read depth and dilution of circulating tumor DNA in the circulation by other cfDNA species. In addition to known melanoma driver mutations, several other melanoma-associated mutations were found to be concordant between matched gDNA and cfDNA. This study highlights that WES of cfDNA can capture clinically-relevant mutations present in melanoma metastases, but does not appear to provide any additional unique information on tumor heterogeneity. Targeted deep sequencing may be required to detect low frequency genomic aberrations known for predicting therapy resistance.

Keywords: whole exome sequencing; melanoma; circulating tumor DNA

Peer-reviewed version available at Cancers 2019, 11, 1905; doi:10.3390/cancers11121905

1. Introduction

Analysis of circulating tumor DNA (ctDNA) can be used to identify therapeutically actionable mutations, monitor disease progression, detect residual disease and track the genomic evolution of treatment resistance [1-4]. The genomic profiling of ctDNA using whole genome, whole exome or targeted sequencing is feasible, but technically challenging due to the low quantities and fragmented nature of ctDNA [5-8]. Moreover, ctDNA and tumor genomic (g) DNA are rarely analysed together, although a few reports comparing whole exome sequencing (WES) of gDNA and ctDNA using matched tissue and blood samples in other cancer types have highlighted that ctDNA can capture intra-patient tumor genetic heterogeneity [9-11].

In melanoma, ctDNA has shown significant predictive and prognostic value. Longitudinal ctDNA assessment accurately predicted progression-free survival and overall survival in stage IV melanoma patients treated with BRAF and MEK inhibitors or immunotherapy [12-14] and the melanoma-specific survival of patients with high-risk stage III resected melanoma [15]. ctDNA can also monitor the appearance of treatment-resistant melanoma subclones [13] and differentiate true progression from pseudoprogression in melanoma patients treated with immunotherapy [16]. In the majority of these studies, melanoma ctDNA was evaluated using droplet digital PCR and single mutation detection. Recent studies are now applying whole exome or targeted sequencing to characterize ctDNA, although the value of genomic profiling ctDNA in comparison to genomic melanoma DNA has not been explored.

In this study, we sought to evaluate whether sequencing of ctDNA could yield more comprehensive tumor-mutation profile data compared to sequencing a single melanoma biopsy. WES of gDNA and ctDNA was undertaken using a cohort of patients with metastatic melanoma using matched tissue and blood samples.

2. Results

2.1. Patient Cohort

Ten patients with metastatic melanoma with established driver BRAF or NRAS mutations were included in this study; 5/10 patients were aged 65 years or older, 8/10 were male and 6/10 with American Joint Committee on Cancer (AJCC) stage M1c disease [17] (Table 1). Time between tissue and liquid biopsy was less than 6 months in all patients (median 2.75 months, range 1-6 months), and three patients each had tissue and liquid biopsy collected concurrently. Samples were collected prior to systemic treatment, i.e pre-treatment (PRE) or at time of progression on treatment (PROG). Systemic treatments included the immune checkpoint inhibitors ipilimumab, nivolumab and pembrolizumab and the targeted therapies, dabrafenib and trametinib.

2.2. WES and droplet digital PCR

The amount of tumor tissue gDNA extracted for this study was in the μg range and significantly higher than the ng amounts of extracted plasma circulating cell-free DNA (cfDNA) (Table S1). Nevertheless, sequencing libraries were successfully generated for ctDNA and gDNA for each patient, and WES output based on total reads and coverage was not significantly different when comparing gDNA and cfDNA (Figure 1A and B). However, the mean read depth was found to be significantly less for cfDNA, presumably due to the lower amounts of cfDNA template available for sequencing (Figure 1C). This was not always the case however, with higher cfDNA compared to gDNA mean read depth for patients 4 and 9 (Figure 1C).

Peer-reviewed version available at Cancers 2019, 11, 1905; doi:10.3390/cancers11121905

Table 1. Patient, treatment and biopsy characteristics.

Patient	Age (years)	Sex	Tumor biopsy site	Current treatment when tissue biopsy procured	Current treatment when liquid biopsy procured	Time between biopsies (months)*	Mutation	Stage (AJCC 8th ed [18])	Serum LDH**	OS (months)
1	76	M	Brain	PROG pembro	PROG pembro	Concurrent	BRAF V600E NRAS Q22K	M1d	NA	4.8
2	61	F	Inguinal LN	PROG combi-DT	PROG combi-DT	6	BRAF V600E	M1c	< ULN	Alive (33.7)
3	58	M	Brain	PRE nivo	PROG nivo	2	BRAF V600E	M1d	> 2x ULN	19.2
4	48	M	Thigh SC	PROG ipi + nivo	PROG ipi + nivo	1	BRAF V600E	M1d	< ULN	20.7
5	56	M	Inguinal LN	PRE combi-DT	PROG combi-DT	4	BRAF V600K	M1c	> 2x ULN	10.4
6	70	M	Liver	PRE nivo	PRE nivo	Concurrent	BRAF G466E	M1d	> 2x ULN	1.2
7	37	F	Ovary	PROG ipi + pembro	PROG ipi + pembro	4	NRAS Q61K	M1c	> 1x ULN	25.7
8	65	M	Abdominal LN	PROG ipi + pembro	PROG ipi + pembro	Concurrent	NRAS Q61K	M1c	< ULN	Alive (52.2)
9	65	M	Liver	PROG nivo	PROG nivo	3	NRAS Q61R	M1c	> 1x ULN	20.4
10	69	M	Brain	PRE pembro	PROG pembro	6	NRAS Q61R	M1c	< ULN	11.6

*In patients 2, 3, 4, 5 and 10, tumor biopsies were taken prior to the liquid biopsies and in patients 7 and 9 tumor biopsies were taken after the liquid biopsies

**Taken at time of liquid biopsy

AJCC, American Joint Committee on Cancer; F, female; M, male; OS, overall survival; ULN, upper limit of normal; NA, not available; LN, lymph node; SC, subcutaneous; LN, lymph node; PRE, prior to systemic therapy; PROG, at time of progression on treatment; nivo, nivolumab (anti-PD1); pembro, pembrolizumab (anti-PD1); ipi, ipilimumab (anti-CTLA4); combi-DT, combination dabrafenib (BRAF inhibitor) and trametinib (MEK inhibitor)

Peer-reviewed version available at Cancers 2019, 11, 1905; doi:10.3390/cancers11121905

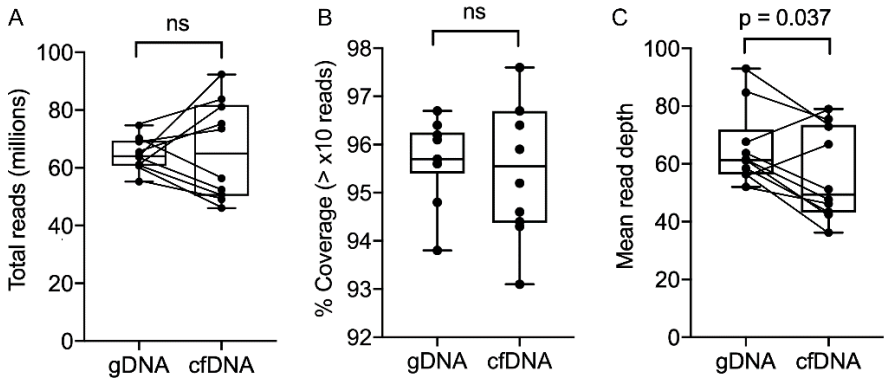

Figure 1. Summary of WES analysis. Comparison of (**A**) total reads, (**B**) % coverage (>10x reads) and (**C**) mean read depth for matched (connected by lines) genomic (g) DNA and circulating cell-free (cf) DNA from advanced melanoma patients. Plots show median with interquartile ranges and data were compared using the paired, nonparametric Wilcoxon test. ns, not significant.

We also examined the relationship between ctDNA and cfDNA quantities in the 10 melanoma patients, by measuring the amount of ctDNA using highly sensitive droplet digital PCR. We found that ctDNA copy number significantly correlated with total extracted cfDNA (Figure S1).

2.3. *Single nucleotide variant analysis*

A list of single nucleotide variants (SNVs) was generated from matched gDNA and cfDNA WES. Non-synonymous and synonymous SNVs with mutant allele frequency (MAF) ≥ 20% were included (summarized in Table S2). There was no significant difference in the total number of SNVs in the patient-matched tumor gDNA and cfDNA and no difference in the derived tumor mutation burden determined from WES of either gDNA or cfDNA (Figure 2).

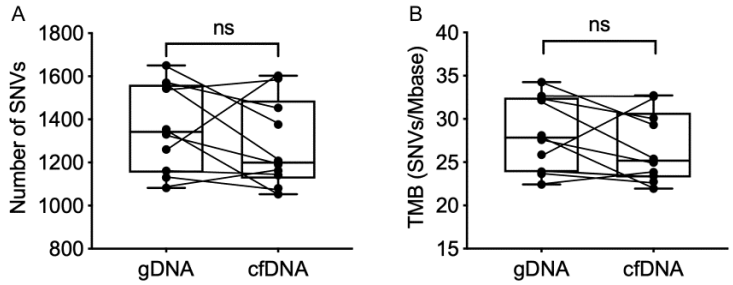

Figure 2. Comparison of the mutational load for melanoma patient matched (connected by lines) genomic (g) DNA and circulating cell-free (cf) DNA analysed by WES. (**A**) Total number of filtered SNVs. (**B**) Tumor mutational burden (TMB). The filtered list of SNVs was produced from the WES list of total SNPs using Ingenuity Variant Analysis as described in Materials and Methods. The TMB was calculated as described in Materials and Methods. Plots show median with interquartile ranges and data were compared using the paired, nonparametric Wilcoxon test. Abbreviations: n.s, not significant.

The degree of overlap or concordance of SNVs for gDNA and cfDNA from matched patient samples ranged from 55-72%, with the total number of SNVs (gDNA plus cfDNA) ranging from 1324-1837 (Figure 3). Similar percentages of SNVs were unique to either gDNA (range 11-31%) or cfDNA (range 10-30%) (Figure 3). Overall, there was no detectable difference in the degree of overlap of SNVs in matched gDNA and cfDNA from individual patients regardless of treatment type (naïve, combination dabrafenib and trametinib (combi-DT) or immune checkpoint therapy), response to treatment, timing of biopsies or location of the biopsied tumor (Table 1). Moreover, the three patients with concurrent tissue and liquid biospies displayed a wide range of SNV overlap (55% in patient 8, 60% in patient 6 and 72% in patient 1).

Peer-reviewed version available at Cancers 2019, 11, 1905; doi:10.3390/cancers11121905

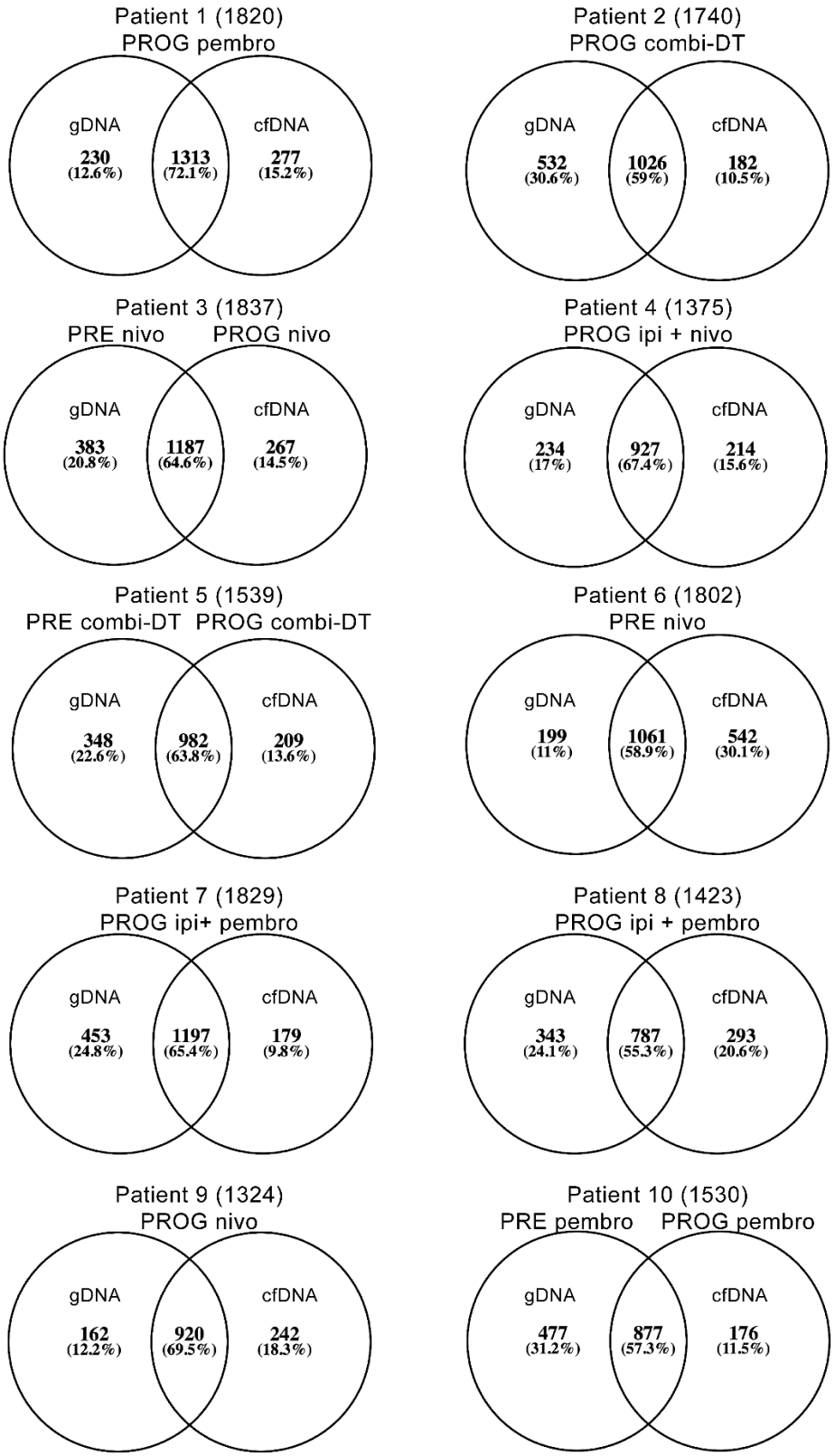

Figure 3. Degree of SNV overlap for patient matched genomic (g) DNA and circulating cell-free (cf) DNA as identified by WES. The filtered list of SNVs was produced from the WES list of total SNPs using an Ingenuity Variant Analysis as described in Materials and Methods. The numbers in parentheses represent total combined SNVs. PRE, prior to systemic therapy; PROG, at time of progression on treatment; nivo, nivolumab (anti-PD1); pembro, pembrolizumab (anti-PD1); ipi, ipilimumab (anti-CTLA4); combi-DT, combination dabrafenib (BRAF inhibitor) and trametinib (MEK inhibitor).

Peer-reviewed version available at Cancers 2019, 11, 1905; doi:10.3390/cancers11121905

2.4. Mutant allele frequency (MAF) of single nucleotide variants

The MAFs for the shared SNVs in patient-matched gDNA and cfDNA showed significant correlation in all patients, with the highest level of correlation between gDNA and cfDNA observed in patients 6 and 9 (Figure 4 and S2). Interestingly, both patients had gDNA derived from core liver biopsies (Table 1), and the high concordance between circulating and liver melanoma SNVs may reflect the fact the liver melanoma metastases tend to be larger than melanoma metastases in other sites, including brain, soft tissue and lung [19].

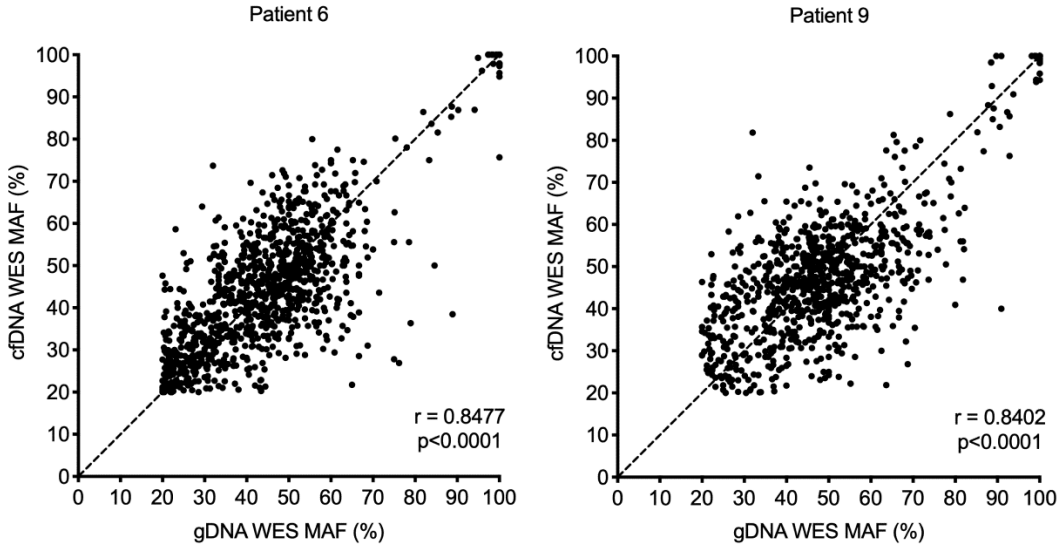

Figure 4. Degree of Pearson correlation between the MAF of SNVs common to patient matched genomic (g) DNA and circulating cell-free (cf) DNA as identified by WES. Dotted line indicates y=x.

2.5. Melanoma driver mutations

We then focused on the *BRAF* and *NRAS* melanoma driver gene mutations (Table 1). WES of gDNA was able to identify the driver mutations in all patients (MAF range 25-83%), whereas WES of cfDNA only detected the driver mutation in six of ten patients (patients 1, 3, 5, 6, 7 and 9) when applying a MAF cutoff of at least 20% (Table S3). However, the cfDNA driver mutations were detected by manual curation in the remaining four patients (patients 2, 4, 8 and 10; MAF 7-12%), and were well below the gDNA MAF and below the MAF cut-off of 20% (Table S3). Comparison of the driver MAF determined by WES of gDNA versus cfDNA across all 10 patients showed no significant correlation (Figure 5A). All driver MAFs in cfDNA were independently validated; nine using droplet digital (dd) PCR analysis and one using highly sensitive targeted sequencing analysis (Table S3). There was significant correlation between MAF based on WES and ddPCR/targeted NGS sequencing of cfDNA (Figure 5B). However, there was less correlation (though still significant) when the driver MAF based on WES of gDNA and ddPCR analysis of cfDNA was compared (Figure 5C). This highlights that melanoma driver MAF captured in cfDNA is generally lower than the driver MAF from gDNA, consistent with our observation that MAF of common SNVs was generally lower in cfDNA WES compared to patient-matched gDNA WES data (Figure 4 and S2).

Peer-reviewed version available at Cancers 2019, 11, 1905; doi:10.3390/cancers11121905

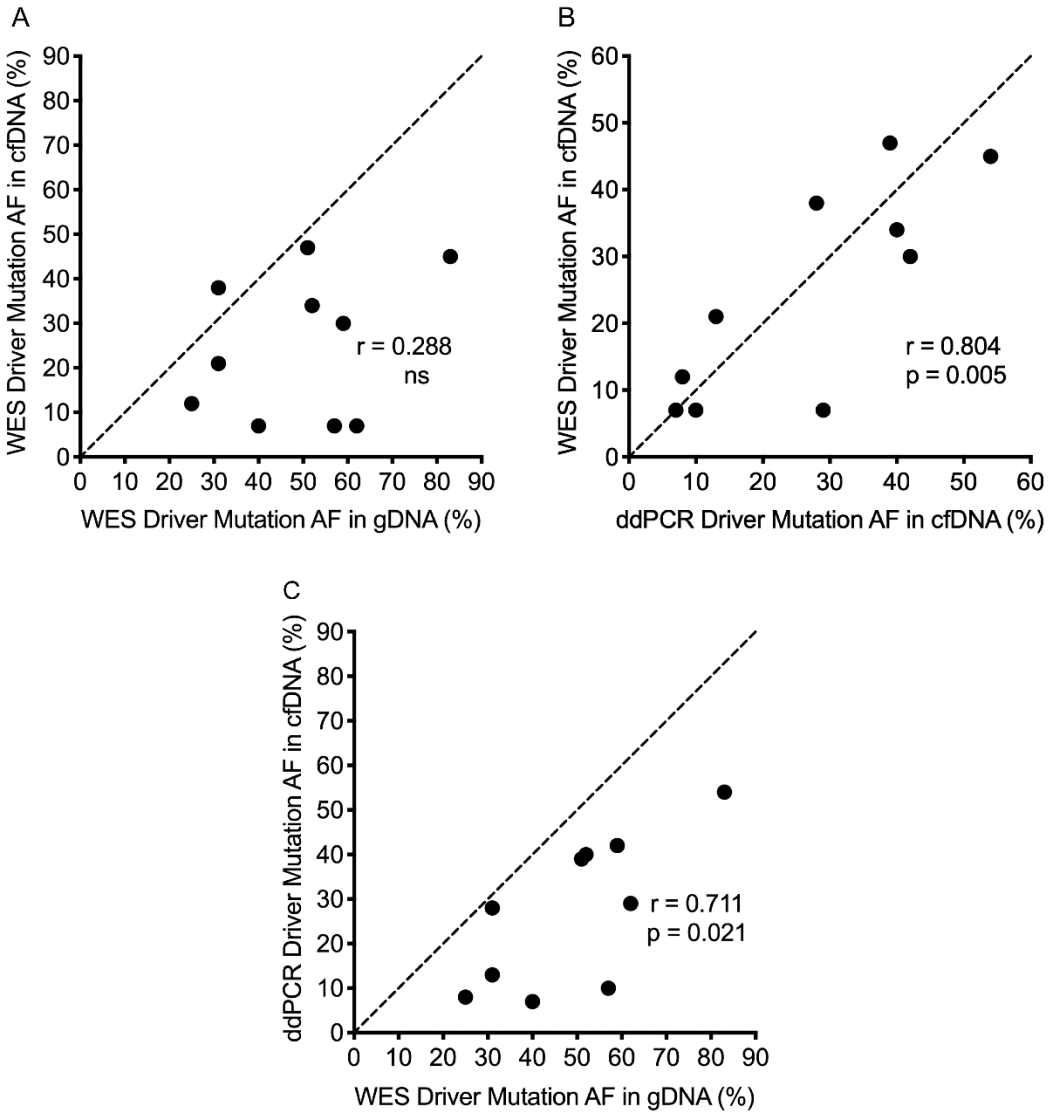

Figure 5. Degree of Pearson correlation based on the mutant allele frequency of the driver mutation in melanoma patients. (**A**) WES of genomic (g) DNA versus WES of circulating cell-free (cf) DNA. (**B**) ddPCR analysis of cfDNA versus WES of cfDNA. (**C**) WES of gDNA versus ddPCR analysis of cfDNA. ns, not significant.

2.6. *Other highlighted mutations*

In addition to mutations in the *BRAF* or *NRAS* genes, we identified other melanoma-associated mutations in the WES dataset (Table S4). These mutations were detected initially in either gDNA, cfDNA or both. SNVs unique to either gDNA or cfDNA were subsequently found by manual curation of WES Bam files to occur in both sources of DNA (Table S4). Only one mutation, MASP2 R356W, was found to be unique to cfDNA in patient 6 (Table S4). Interestingly, patient 6, the only treatment naïve patient, had the highest number of melanoma-associated mutations (Table S4), although he did not have the highest number of total SNVs (Figure 3). The CDK4 R24C mutation in the $BRAF^{V600E}$ mutant patient 3 was the only additional melanoma-associated mutation predicted to be a driver mutation (Table S4). Rare germline mutations in CDK4 at position 24 predispose to melanoma susceptibility [20]. We identified an NRAS Q22K mutation in patient 1 (Table S4). Although this is an uncommon NRAS variant, it has been reported in a small number of tumors including melanoma [21]. It potently induces MAPK signaling [22] and may have contributed to BRAF/MEK inhibitor resistance in the tumor (Table 1).

Peer-reviewed version available at Cancers 2019, 11, 1905; doi:10.3390/cancers11121905

3. Discussion

In this study we compared WES of matched gDNA and cfDNA from 10 patients with metastatic melanoma in both treatment naïve patients and patients on systemic molecular or immune therapies. We now report that cfDNA sequencing provides an accurate, albeit incomplete snapshot of the mutation profile and mutation burden of the patient-matched metastatic tumor. The SNVs found in the patient-matched melanoma gDNA and ctDNA overlapped by 55 to 72%, which is comparable to gDNA and cfDNA mutation concordance data reported for other cancers [9,10,23]. Importantly, cfDNA mutation profiling provided an accurate mutation profile irrespective of the site of the patient-matched tumor and this was particularly important for brain metastases, given that levels of ctDNA derived from brain metastases are extremely low, possibly as a result of the blood-brain barrier [14,24]. It is likely that ctDNA in these melanoma patients is derived from extracranial tumors, and ctDNA remained informative for brain melanoma because melanoma brain tumors have similar mutational and treatment response profiles to concurrent extracranial tumors [25-29]. It is also worth noting that MAFs of common SNV were most concordant between cfDNA and liver melanoma metastases.

Although we did observe consistently lower MAFs for SNVs in cfDNA compared to gDNA, this is presumably due to the combination of lower read depth for cfDNA and the fact that ctDNA makes up only a fraction of cfDNA [30]. We also applied a MAF threshold of at least 20% to define variants in the gDNA and cfDNA sequencing data, as suggested previously [10]. In some samples, a lower MAF threshold was required to detect the *BRAF* and *NRAS* driver mutations and allele frequency thresholds need to be optimized for sensitivity and specificity with larger cohort studies. Although, ddPCR analysis of cfDNA was more sensitive that WES cfDNA sequencing, the additional information gained by unbiased sequencing, including tumor mutation burden, which is associated with clinical benefit for immunotherapy [23] and the potential to define resistant subclones is an important advantage. For instance, we identified an activating and putative resistance *NRAS* mutation (Q22K) in both gDNA and cfDNA in a BRAF-mutant melanoma after progression on combined BRAF and MEK inhibitors [31]. There is also significant scope to improve the sensitivity of cfDNA sequencing with multi-gene panels, molecular barcoding and size selection enrichment.

In conclusion, WES analysis of total SNVs in cfDNA provides an accurate snapshot of the mutation landscape and burden of melanoma metastases, although additional improvements in sensitivity are required for the accurate profiling of smaller-sized descendent tumor subclones. This may be clinically important as pre-existing variants capable of promoting treatment resistance may cause a fitness deficit and produce only minor descendent clones in the absence of selective pressure. This appears to be the case, for instance, for $BRAF^{V600E}$ gene amplification, a common mediator of resistance to BRAF and MEK inhibitors [32], which also promotes proliferative arrest in the absence of MAPK inhibitors. Thus, the use of cfDNA to identify the tumor metagenome (i.e. the aggregate of co-existent tumor subclones) will require sequencing depth that allows the detection of 0.1% MAF afforded by targeted gene panels [33,34]. At this MAF threshold, ctDNA is detectable in 75% of metastatic melanoma patients [12] and improving the sensitivity of cfDNA sequencing promises significant benefits, especially as a predictive biomarkers in an era with many effective therapies.

4. Materials and Methods

4.1. Human melanoma samples

The fresh-frozen tissue and blood samples used in the current study were obtained from the Melanoma Institute Australia biospecimen bank with written informed patient consent and institutional review board approval (Sydney Local Health District Human Research Ethics Committee, Protocol No. X15–0454 and HREC/11/RPAH/444). All samples were pathologically assessed prior to inclusion into the study, as previously described [35].

Blood (10 ml) was collected in EDTA tubes (Becton Dickinson, USA) and processed immediately. Tubes were spun at 800 *g* for 15 min at room temperature. Plasma was then removed into new 15 ml

Peer-reviewed version available at Cancers 2019, 11, 1905; doi:10.3390/cancers11121905

tubes without disturbing the buffy coat and respun at 1600 *g* for 10 min at room temperature to remove cellular debris. Plasma was stored in 1 ml aliquots at -80°C.

4.2. DNA extractions

Tumor-derived gDNA for WES was extracted from fresh-frozen tissue using the DNeasy Blood and Tissue Kit (Qiagen) according to the manufacturer's instructions. Plasma cfDNA from melanoma patients was purified using the QIAamp circulating nucleic acid kit (Qiagen) according to the manufacturer's instructions. cfDNA was purified from 3-5 ml of plasma and the final elution volume was 30-40 µl.

4.3 Analysis of purified cfDNA from plasma

The copy number of cfDNA extracted from plasma was analysed as previously described [14]. The QX200 ddPCR system was used to detect mutant *NRAS* or *BRAF* as previously described (Bio-Rad) [14]. The copy number was determined with Quantasoft software version 1.7.4 (BioRad) using a manual threshold setting. One patient cfDNA sample was analysed by Thermofisher Scientific Australia using their lung oncomine cfDNA assay according to the manufacturer's instructions.

4.4. Whole exome sequencing

Exome library preparation and sequencing workflow utilised the SureSelect V5-post capture kit (Agilent) and Illumina HiSeq 4000 platform and was performed by the Macrogen corporation. Total DNA was quantified using a Quant-iT Picogreen dsDNA assay kit (Life Technologies). The size of sequencing library preparations was ascertained on a 2100 Bioanalyzer (Agilent) using a DNA 1000 chip. The quantity of individual sequencing libraries was determined using qPCR quantification (Illumina) according to the manufacturer's instructions. Sequencing reads were mapped using Burrows-Whole Aligner (BWA) [36] against the human reference genome hg19 (https://genome.ucsc.edu). SNPs were detected using SAMTools [37], variant database dbSNP [38] and 1000 genomes project [39].

4.5. Filtered single nucleotide variants

Filtered SNV annotation and interpretation analyses were generated through the use of Ingenuity Variant Analysis software https://www.qiagenbioinformatics.com/products/ingenuity-variant-analysis from QIAGEN, Inc. Included SNVs were those with a call quality of at least 20, a read depth of at least 10 and a minimal MAF of 20%. Included SNVs were also those outside the top 1.0% most exonically variable genes in healthy public genomes (1000 genomes project [39]). Excluded SNVs that were likely to be polymorphisms were those observed with an allele frequency greater than or equal to 3.0% of the genomes in the 1000 genomes project [39] or greater than or equal to 3.0% of the NHLBI ESP exomes [40] or greater than or equal to 3.0% of the ExAC frequency [41] or greater than or equal to 3.0% of the gnomAD frequency [41]. Further manual filtering consisted of including only exonic SNVs that were either non-synonymous mutations or synonymous mutations with a known cosmic ID. Melanoma-associated mutations were confirmed using cbioportal [42,43] (http://www.cbioportal.org). The tumor mutational burden (SNVs/Mbase) was calculated using a human exome size (Mbase) based on the number of on-target genotypes (with more than 10X sequencing depth) determined for each patient sample subjected to WES and the total number of filtered SNVs.

Peer-reviewed version available at Cancers 2019, 11, 1905; doi:10.3390/cancers11121905

4.6. Statistical analysis

Venn diagrams were generated using the interactive online tool Venny 2.1 http://bioinfogp.cnb.csic.es/tools/venny/index.html. Pearson correlation coefficients were determined using Prism version 8.1.1. A paired, nonparametric Wilcoxon test was also performed using Prism.

5. Conclusions

In this study, we have shown that sequencing of cfDNA to capture the mutational profile and mutation burden of melanoma metastases is a viable option. The sequencing read depth of cfDNA was consistently lower than gDNA, and thus mutation detection sensitivity can be an issue in patients with limited tumour burden or intracranial disease. Although WES was used in the current study, this approach is likely to be superseded by targeted deep sequencing due its greater sensitivity accomplished through greater read depth. This is certainly feasible for melanoma, where a targeted gene panel can be designed to cover the majority of known somatic mutations.

Supplementary Materials: The following are available online at www.mdpi.com/xxx/s1, Figure S1: Total circulating cell-free DNA vs ctDNA copy number, Figure S2: Common SNVs MAF, Table S1: DNA Quantity, Table S2: Filtered SNVs, Table S3: Driver Melanoma Mutations, Table S4: Highlighted SNVs.

Author Contributions: Conceptualization, R.J.D., J.H.L. and H.R.; methodology, R.J.D., J.H.L., and H.R.; formal analysis, R.J.D., J.H.L., D.S., J.Y.H.Y., and H.R.; investigation, R.J.D., J.H.L.; resources, R.F.K., A.M.M., M.S.C., G.V.L, A.J.S, J.R.S, R.P.M.S, J.F.T., S.C. and R.A.S.; writing—original draft preparation, R.J.D., and H.R.; writing—review and editing, R.J.D., J.H.L., D.S., J.Y.H.Y., R.F.K., A.M.M., M.S.C., G.V.L, A.J.S, J.R.S, R.P.M.S., J.F.T., S.C., R.A.S., and H.R.; visualization, R.J.D., J.H.L., and H.R.; supervision, H.R.; project administration, H.R.; funding acquisition, H.R.

Funding: R.J.D. was supported in part by a donation to Melanoma Institute Australia from the Clearbridge Foundation. This work was also supported in part by the National Health and Medical Research Council (APP1093017 and APP1128951). H.R., R.A.S, and G.V.L. are supported by National Health and Medical Research Council Research Fellowships (APP1104503, APP1141295 and APP1119059). G.V.L. and J.F.T. are also supported by the Medical Foundation of The University of Sydney. A.M.M. is supported by a Cancer Institute NSW Fellowship. J.R.S and R.P.M.S are supported by Melanoma Institute Australia. Support from colleagues at Melanoma Institute Australia, the Royal Prince Alfred Hospital and Westmead Hospital is also gratefully acknowledged.

Conflicts of Interest: G.V.L. receives consultant service fees from Amgen, BMS, Array, Pierre-Fabre, Novartis, Merck Sharp & Dohme (MSD), and Roche. A.M.M. is an advisory board member for BMS, MSD, Novartis, Roche, and Pierre Fabre. R.F.K. has been on advisory boards for Roche, Amgen, BMS, MSD, Novartis and TEVA and has received honoraria from MSD, BMS and Novartis. M.S.C. is an advisory board member for MSD, BMS, Novartis, Pierre-Fabre, Roche and Amgen. R.A.S has received honoraria from MSD, Novartis, GSK, BMS, Myriad and NeraCare. J.F.T. has been on advisory boards for GlaxoSmithKline, Provectus Inc, Merck Sharp Dohme and Bristol Myers Squibb and has received honoraria and travel support from GlaxoSmithKline and Provectus Inc. He has received honoraria for advisory board participation from Merck Sharp Dohme and Bristol Myers Squibb. These companies had no role in the design of the study; in the collection, analyses, or interpretation of data; in the writing of the manuscript, or in the decision to publish the results. All remaining authors have declared no conflicts of interest.

References

1. Yi, X.; Ma, J.; Guan, Y.; Chen, R.; Yang, L.; Xia, X. The feasibility of using mutation detection in ctDNA to assess tumor dynamics. *Int J Cancer* **2017**, *140*, 2642-2647, doi:10.1002/ijc.30620.
2. Wan, J.C.M.; Massie, C.; Garcia-Corbacho, J.; Mouliere, F.; Brenton, J.D.; Caldas, C.; Pacey, S.; Baird, R.; Rosenfeld, N. Liquid biopsies come of age: towards implementation of circulating tumour DNA. *Nat Rev Cancer* **2017**, *17*, 223-238, doi:10.1038/nrc.2017.7.

3. De Rubis, G.; Krishnan, S.R.; Bebawy, M. Circulating tumor DNA - Current state of play and future perspectives. *Pharmacol Res* **2018**, *136*, 35-44, doi:10.1016/j.phrs.2018.08.017.
4. Donaldson, J.; Park, B.H. Circulating tumor DNA: Measurement and clinical utility. *Annu Rev Med* **2018**, *69*, 223-234, doi:10.1146/annurev-med-041316-085721.
5. Klevebring, D.; Neiman, M.; Sundling, S.; Eriksson, L.; Darai Ramqvist, E.; Celebioglu, F.; Czene, K.; Hall, P.; Egevad, L.; Gronberg, H., et al. Evaluation of exome sequencing to estimate tumor burden in plasma. *PLoS One* **2014**, *9*, e104417, doi:10.1371/journal.pone.0104417.
6. Ahlborn, L.B.; Rohrberg, K.S.; Gabrielaite, M.; Tuxen, I.V.; Yde, C.W.; Spanggaard, I.; Santoni-Rugiu, E.; Nielsen, F.C.; Lassen, U.; Mau-Sorensen, M., et al. Application of cell-free DNA for genomic tumor profiling: a feasibility study. *Oncotarget* **2019**, *10*, 1388-1398, doi:10.18632/oncotarget.26642.
7. Butler, T.M.; Johnson-Camacho, K.; Peto, M.; Wang, N.J.; Macey, T.A.; Korkola, J.E.; Koppie, T.M.; Corless, C.L.; Gray, J.W.; Spellman, P.T. Exome sequencing of cell-free DNA from metastatic cancer patients identifies clinically actionable mutations distinct from primary disease. *PLoS One* **2015**, *10*, e0136407, doi:10.1371/journal.pone.0136407.
8. Murtaza, M.; Dawson, S.J.; Tsui, D.W.; Gale, D.; Forshew, T.; Piskorz, A.M.; Parkinson, C.; Chin, S.F.; Kingsbury, Z.; Wong, A.S., et al. Non-invasive analysis of acquired resistance to cancer therapy by sequencing of plasma DNA. *Nature* **2013**, *497*, 108-112, doi:10.1038/nature12065.
9. Chicard, M.; Colmet-Daage, L.; Clement, N.; Danzon, A.; Bohec, M.; Bernard, V.; Baulande, S.; Bellini, A.; Deveau, P.; Pierron, G., et al. Whole-exome sequencing of cell-free DNA reveals temporo-spatial heterogeneity and identifies treatment-resistant clones in neuroblastoma. *Clin Cancer Res* **2018**, *24*, 939-949, doi:10.1158/1078-0432.CCR-17-1586.
10. Dietz, S.; Schirmer, U.; Merce, C.; von Bubnoff, N.; Dahl, E.; Meister, M.; Muley, T.; Thomas, M.; Sultmann, H. Low input whole-exome sequencing to determine the representation of the tumor exome in circulating DNA of non-small cell lung cancer patients. *PLoS One* **2016**, *11*, e0161012, doi:10.1371/journal.pone.0161012.
11. Jimenez, I.; Chicard, M.; Colmet-Daage, L.; Clement, N.; Danzon, A.; Lapouble, E.; Pierron, G.; Bohec, M.; Baulande, S.; Berrebi, D., et al. Circulating tumor DNA analysis enables molecular characterization of pediatric renal tumors at diagnosis. *Int J Cancer* **2018**, *Epub*, doi:10.1002/ijc.31620.
12. Santiago-Walker, A.; Gagnon, R.; Mazumdar, J.; Casey, M.; Long, G.V.; Schadendorf, D.; Flaherty, K.; Kefford, R.; Hauschild, A.; Hwu, P., et al. Correlation of BRAF mutation status in circulating-free DNA and tumor and association with clinical outcome across four BRAFi and MEKi clinical trials. *Clin Cancer Res* **2016**, *22*, 567-574, doi:10.1158/1078-0432.CCR-15-0321.
13. Gray, E.S.; Rizos, H.; Reid, A.L.; Boyd, S.C.; Pereira, M.R.; Lo, J.; Tembe, V.; Freeman, J.; Lee, J.H.; Scolyer, R.A., et al. Circulating tumor DNA to monitor treatment response and detect acquired resistance in patients with metastatic melanoma. *Oncotarget* **2015**, *6*, 42008-42018, doi:10.18632/oncotarget.5788.
14. Lee, J.H.; Long, G.V.; Boyd, S.; Lo, S.; Menzies, A.M.; Tembe, V.; Guminski, A.; Jakrot, V.; Scolyer, R.A.; Mann, G.J., et al. Circulating tumour DNA predicts response to anti-PD1 antibodies in metastatic melanoma. *Ann Oncol* **2017**, *28*, 1130-1136, doi:10.1093/annonc/mdx026.
15. Lee, J.H.; Saw, R.P.; Thompson, J.F.; Lo, S.; Spillane, A.J.; Shannon, K.F.; Stretch, J.R.; Howle, J.; Menzies, A.M.; Carlino, M.S., et al. Pre-operative ctDNA predicts survival in high-risk stage III cutaneous melanoma patients. *Ann Oncol* **2019**, *30*, 815-822, doi:10.1093/annonc/mdz075.
16. Lee, J.H.; Long, G.V.; Menzies, A.M.; Lo, S.; Guminski, A.; Whitbourne, K.; Peranec, M.; Scolyer, R.; Kefford, R.F.; Rizos, H., et al. Association between circulating tumor DNA and pseudoprogression in

Peer-reviewed version available at Cancers 2019, 11, 1905; doi:10.3390/cancers11121905

patients with metastatic melanoma treated with anti-programmed cell death 1 antibodies. *JAMA Oncol* **2018**, *4*, 717-721, doi:10.1001/jamaoncol.2017.5332.

17. Gershenwald, J.E.; Scolyer, R.A.; Hess, K.R.; Sondak, V.K.; Long, G.V.; Ross, M.I.; Lazar, A.J.; Faries, M.B.; Kirkwood, J.M.; McArthur, G.A., et al. Melanoma staging: Evidence-based changes in the American Joint Committee on Cancer eighth edition cancer staging manual. *CA Cancer J Clin* **2017**, *67*, 472-492, doi:10.3322/caac.21409.
18. Gershenwald, J.E.; Scolyer, R.A.; Hess, K.R.; Thompson, J.F.; Long, G.V.; Ross, M.I. Melanoma of the skin. In *AJCC cancer staging manual.*, Amin, M.B., Edge, S., Greene, F., Byrd, D.R., Brookland, R.K., Washington, M.K., Gershenwald, J.E., Compton, C.C., Hess, K.R., Sullivan, D.C., et al., Eds. New York: Springer: 2017; pp. 563-585.
19. Silva, I.P.d.; Lo, S.; Quek, C.; Gonzalez, M.; Carlino, M.S.; Long, G.V.; Menzies, A.M. Site-specific response patterns, pseudoprogression, and acquired resistance in patients with melanoma treated with ipilimumab combined with anti–PD-1 therapy. *Cancer* **2019**, Epub.
20. Puntervoll, H.E.; Yang, X.R.; Vetti, H.H.; Bachmann, I.M.; Avril, M.F.; Benfodda, M.; Catricala, C.; Dalle, S.; Duval-Modeste, A.B.; Ghiorzo, P., et al. Melanoma prone families with CDK4 germline mutation: phenotypic profile and associations with MC1R variants. *J Med Genet* **2013**, *50*, 264-270, doi:10.1136/jmedgenet-2012-101455.
21. Hodis, E.; Watson, I.R.; Kryukov, G.V.; Arold, S.T.; Imielinski, M.; Theurillat, J.P.; Nickerson, E.; Auclair, D.; Li, L.; Place, C., et al. A landscape of driver mutations in melanoma. *Cell* **2012**, *150*, 251-263, doi:10.1016/j.cell.2012.06.024.
22. Loree, J.M.; Miron, B.; Holla, V.; Overman, M.J.; Pereira, A.A.L.; Lam, M.; Morris, V.K.; Raghav, K.P.S.; Routbort, M.; Shaw, K.R., et al. Not all RAS mutations created equal: Functional and clinical characterization of 80 different KRAS and NRAS mutations. *Journal of Clinical Oncology* **2017**, *35*, 3589-3589, doi:10.1200/JCO.2017.35.15_suppl.3589.
23. Koeppel, F.; Blanchard, S.; Jovelet, C.; Genin, B.; Marcaillou, C.; Martin, E.; Rouleau, E.; Solary, E.; Soria, J.C.; Andre, F., et al. Whole exome sequencing for determination of tumor mutation load in liquid biopsy from advanced cancer patients. *PLoS One* **2017**, *12*, e0188174, doi:10.1371/journal.pone.0188174.
24. De Mattos-Arruda, L.; Mayor, R.; Ng, C.K.Y.; Weigelt, B.; Martinez-Ricarte, F.; Torrejon, D.; Oliveira, M.; Arias, A.; Raventos, C.; Tang, J., et al. Cerebrospinal fluid-derived circulating tumour DNA better represents the genomic alterations of brain tumours than plasma. *Nat Commun* **2015**, *6*, 8839, doi:10.1038/ncomms9839.
25. Fischer, G.M.; Jalali, A.; Kircher, D.A.; Lee, W.C.; McQuade, J.L.; Haydu, L.E.; Joon, A.Y.; Reuben, A.; de Macedo, M.P.; Carapeto, F.C.L., et al. Molecular profiling reveals unique immune and metabolic features of melanoma brain metastases. *Cancer Discov* **2019**, *9*, 628-645, doi:10.1158/2159-8290.CD-18-1489.
26. Long, G.V.; Atkinson, V.; Lo, S.; Sandhu, S.; Guminski, A.D.; Brown, M.P.; Wilmott, J.S.; Edwards, J.; Gonzalez, M.; Scolyer, R.A., et al. Combination nivolumab and ipilimumab or nivolumab alone in melanoma brain metastases: a multicentre randomised phase 2 study. *Lancet Oncol* **2018**, *19*, 672-681, doi:10.1016/S1470-2045(18)30139-6.
27. Davies, M.A.; Saiag, P.; Robert, C.; Grob, J.J.; Flaherty, K.T.; Arance, A.; Chiarion-Sileni, V.; Thomas, L.; Lesimple, T.; Mortier, L., et al. Dabrafenib plus trametinib in patients with BRAF(V600)-mutant melanoma brain metastases (COMBI-MB): a multicentre, multicohort, open-label, phase 2 trial. *Lancet Oncol* **2017**, *18*, 863-873, doi:10.1016/S1470-2045(17)30429-1.

28. Long, G.V.; Trefzer, U.; Davies, M.A.; Kefford, R.F.; Ascierto, P.A.; Chapman, P.B.; Puzanov, I.; Hauschild, A.; Robert, C.; Algazi, A., et al. Dabrafenib in patients with Val600Glu or Val600Lys BRAF-mutant melanoma metastatic to the brain (BREAK-MB): a multicentre, open-label, phase 2 trial. *Lancet Oncol* **2012**, *13*, 1087-1095, doi:10.1016/S1470-2045(12)70431-X.

29. Tawbi, H.A.; Forsyth, P.A.; Algazi, A.; Hamid, O.; Hodi, F.S.; Moschos, S.J.; Khushalani, N.I.; Lewis, K.; Lao, C.D.; Postow, M.A., et al. Combined nivolumab and ipilimumab in melanoma metastatic to the brain. *N Engl J Med* **2018**, *379*, 722-730, doi:10.1056/NEJMoa1805453.

30. Calapre, L.; Warburton, L.; Millward, M.; Ziman, M.; Gray, E.S. Circulating tumour DNA (ctDNA) as a liquid biopsy for melanoma. *Cancer Lett* **2017**, *404*, 62-69, doi:10.1016/j.canlet.2017.06.030.

31. Johnson, D.B.; Menzies, A.M.; Zimmer, L.; Eroglu, Z.; Ye, F.; Zhao, S.; Rizos, H.; Sucker, A.; Scolyer, R.A.; Gutzmer, R., et al. Acquired BRAF inhibitor resistance: A multicenter meta-analysis of the spectrum and frequencies, clinical behaviour, and phenotypic associations of resistance mechanisms. *Eur J Cancer* **2015**, *51*, 2792-2799, doi:10.1016/j.ejca.2015.08.022.

32. Long, G.V.; Fung, C.; Menzies, A.M.; Pupo, G.M.; Carlino, M.S.; Hyman, J.; Shahheydari, H.; Tembe, V.; Thompson, J.F.; Saw, R.P., et al. Increased MAPK reactivation in early resistance to dabrafenib/trametinib combination therapy of BRAF-mutant metastatic melanoma. *Nat Commun* **2014**, *5*, 5694, doi:10.1038/ncomms6694.

33. Diefenbach, R.J.; Lee, J.H.; Rizos, H. Monitoring melanoma using circulating free DNA. *Am J Clin Dermatol* **2019**, *20*, 1-12, doi:10.1007/s40257-018-0398-x.

34. Calapre, L.; Giardina, T.; Robinson, C.; Reid, A.L.; Al-Ogaili, Z.; Pereira, M.R.; McEvoy, A.C.; Warburton, L.; Hayward, N.K.; Khattak, M.A., et al. Locus-specific concordance of genomic alterations between tissue and plasma circulating tumor DNA in metastatic melanoma. *Mol Oncol* **2019**, *13*, 171-184, doi:10.1002/1878-0261.12391.

35. Hayward, N.K.; Wilmott, J.S.; Waddell, N.; Johansson, P.A.; Field, M.A.; Nones, K.; Patch, A.M.; Kakavand, H.; Alexandrov, L.B.; Burke, H., et al. Whole-genome landscapes of major melanoma subtypes. *Nature* **2017**, *545*, 175-180, doi:10.1038/nature22071.

36. Li, H.; Durbin, R. Fast and accurate short read alignment with Burrows-Wheeler transform. *Bioinformatics* **2009**, *25*, 1754-1760, doi:10.1093/bioinformatics/btp324.

37. Li, H.; Handsaker, B.; Wysoker, A.; Fennell, T.; Ruan, J.; Homer, N.; Marth, G.; Abecasis, G.; Durbin, R.; Genome Project Data Processing, S. The sequence alignment/map format and SAMtools. *Bioinformatics* **2009**, *25*, 2078-2079, doi:10.1093/bioinformatics/btp352.

38. Sherry, S.T.; Ward, M.H.; Kholodov, M.; Baker, J.; Phan, L.; Smigielski, E.M.; Sirotkin, K. dbSNP: the NCBI database of genetic variation. *Nucleic Acids Res* **2001**, *29*, 308-311, doi:10.1093/nar/29.1.308.

39. Genomes Project, C.; Auton, A.; Brooks, L.D.; Durbin, R.M.; Garrison, E.P.; Kang, H.M.; Korbel, J.O.; Marchini, J.L.; McCarthy, S.; McVean, G.A., et al. A global reference for human genetic variation. *Nature* **2015**, *526*, 68-74, doi:10.1038/nature15393.

40. Fu, W.; O'Connor, T.D.; Jun, G.; Kang, H.M.; Abecasis, G.; Leal, S.M.; Gabriel, S.; Rieder, M.J.; Altshuler, D.; Shendure, J., et al. Analysis of 6,515 exomes reveals the recent origin of most human protein-coding variants. *Nature* **2013**, *493*, 216-220, doi:10.1038/nature11690.

41. Lek, M.; Karczewski, K.J.; Minikel, E.V.; Samocha, K.E.; Banks, E.; Fennell, T.; O'Donnell-Luria, A.H.; Ware, J.S.; Hill, A.J.; Cummings, B.B., et al. Analysis of protein-coding genetic variation in 60,706 humans. *Nature* **2016**, *536*, 285-291, doi:10.1038/nature19057.

Peer-reviewed version available at *Cancers* **2019**, *11*, 1905; doi:10.3390/cancers11121905

42. Gao, J.; Aksoy, B.A.; Dogrusoz, U.; Dresdner, G.; Gross, B.; Sumer, S.O.; Sun, Y.; Jacobsen, A.; Sinha, R.; Larsson, E., et al. Integrative analysis of complex cancer genomics and clinical profiles using the cBioPortal. *Sci Signal* **2013**, *6*, pl1, doi:10.1126/scisignal.2004088.

43. Cerami, E.; Gao, J.; Dogrusoz, U.; Gross, B.E.; Sumer, S.O.; Aksoy, B.A.; Jacobsen, A.; Byrne, C.J.; Heuer, M.L.; Larsson, E., et al. The cBio cancer genomics portal: an open platform for exploring multidimensional cancer genomics data. *Cancer Discov* **2012**, *2*, 401-404, doi:10.1158/2159-8290.CD-12-0095.